OPEN ACCESS

GAVIN PUBLISHERS

Current Trends in Nanotechnology

Alkhidir KEME. Curr Trends Nanotechnol 1: 103.
DOI: 10.29011/CTNT-103.100003

Research Article

Luminous Efficacy Fractal Dimension for Characterizing Shajara Reservoirs of the Permo-Carboniferous Shajara Formation, Saudi Arabia

Khalid Elyas Mohamed Elameen Alkhidir*

Department of Petroleum and Natural Gas Engineering, College of Engineering, King Saud University, Saudi Arabia

***Corresponding author:** Khalid Elyas Mohamed Elameen Alkhidir, Department of Petroleum and Natural Gas Engineering, College of Engineering, King Saud University, Saudi Arabia. Tel: +966114679118; Email: kalkhidir@ksu.edu.sa

Citation: Alkhidir KEME (2019) Luminous Efficacy Fractal Dimension for Characterizing Shajara Reservoirs of the Permo-Carboniferous Shajara Formation, Saudi Arabia. Curr Trends Nanotechnol 1: 103. DOI: 10.29011/CTNT-103.100003

Received Date: 04 July 2019; **Accepted Date:** 04 September 2019; **Published Date:** 10 September, 2019

Abstract

The quality and assessment of a reservoir can be documented in details by the application of luminous efficacy. This research aims to calculate fractal dimension from the relationship among luminous efficacy, maximum luminous efficacy and wetting phase saturation and to approve it by the fractal dimension derived from the relationship among capillary pressure and wetting phase saturation. Two equations for calculating the fractal dimensions have been employed. The first one describes the functional relationship between wetting phase saturation, luminous efficacy, maximum luminous efficacy and fractal dimension. The second equation implies to the wetting phase saturation as a function of capillary pressure and the fractal dimension. Two procedures for obtaining the fractal dimension have been utilized. The first procedure was done by plotting the logarithm of the ratio between luminous efficacy and maximum luminous efficacy versus logarithm wetting phase saturation. The slope of the first procedure = 3- Df (Fractal Dimension). The second procedure for obtaining the fractal dimension was determined by plotting the logarithm of capillary pressure versus the logarithm of wetting phase saturation. The slope of the second procedure = Df -3. On the basis of the obtained results of the fabricated stratigraphic column and the attained values of the fractal dimension, the sandstones of the Shajara reservoirs of the Shajara Formation were divided here into three units.

Keywords: Capillary Pressure Fractal Dimension; Luminous Efficacy Fractal Dimension; Shajara Formation; Shajara Reservoirs

Introduction

Seismo electric effects related to electro kinetic potential, dielectric permittivity, pressure gradient, fluid viscosity, and electric conductivity was first reported by [1]. Capillary pressure follows the scaling law at low wetting phase saturation was reported by [2]. Seismo electric phenomenon by considering electro kinetic coupling coefficient as a function of effective charge density, permeability, fluid viscosity and electric conductivity was reported by [3]. The magnitude of seismo electric current depends on porosity, pore size, zeta potential of the pore surfaces, and elastic properties of the matrix was investigated by [4]. The tangent of the ratio of converted electric field to pressure is approximately in inverse proportion to permeability was studied by [5]. Permeability inversion from seismoelectric log at low frequency was studied by [6]. They reported that, the tangent of the ratio among electric excitation intensity and pressure field is a function of porosity, fluid viscosity, frequency, tortuosity, fluid density and Dracy permeability. A decrease of seismo electric frequencies with increasing water content was reported by [7]. An increase of seismo electric transfer function with increasing water saturation was studied by [8]. An increase of dynamic seismo electric transfer function with decreasing fluid conductivity was described by [9]. The amplitude of seismo electric signal increases with increasing permeability which means that the seismo electric effects are directly related to the permeability and can be used to study the permeability of the reservoir was illustrated by [10]. Seismo electric coupling is frequency dependent and decreases expontialy when frequency increases were demonstrated by [11]. An increase of permeability with increasing pressure head and bubble pressure fractal dimension was reported by [12,13]. An increase of geometric relaxation time of induced polarization fractal dimension with permeability increasing and grain size was described by [14,15].

Materials and Methods

Sandstone samples were collected from the surface type section of the Permo-Carboniferous Shajara Formation, latitude 26° 52' 17.4", longitude 43° 36' 18" (Figure1). Porosity was measured on collected samples using mercury intrusion Porosimetry and

permeability was derived from capillary pressure data. The purpose of this paper is to obtain luminous efficacy fractal dimension and to confirm it by capillary pressure fractal dimension. The fractal dimension of the first procedure is determined from the positive slope of the plot of logarithm of the ratio of luminous efficacy to maximum luminous efficacy log ($Le^{1/2}/Le^{1/2}_{max}$) versus log wetting phase saturation (logSw). Whereas the fractal dimension of the second procedure is determined from the negative slope of the plot of logarithm of log capillary pressure (log Pc) versus logarithm of wetting phase saturation (log Sw).

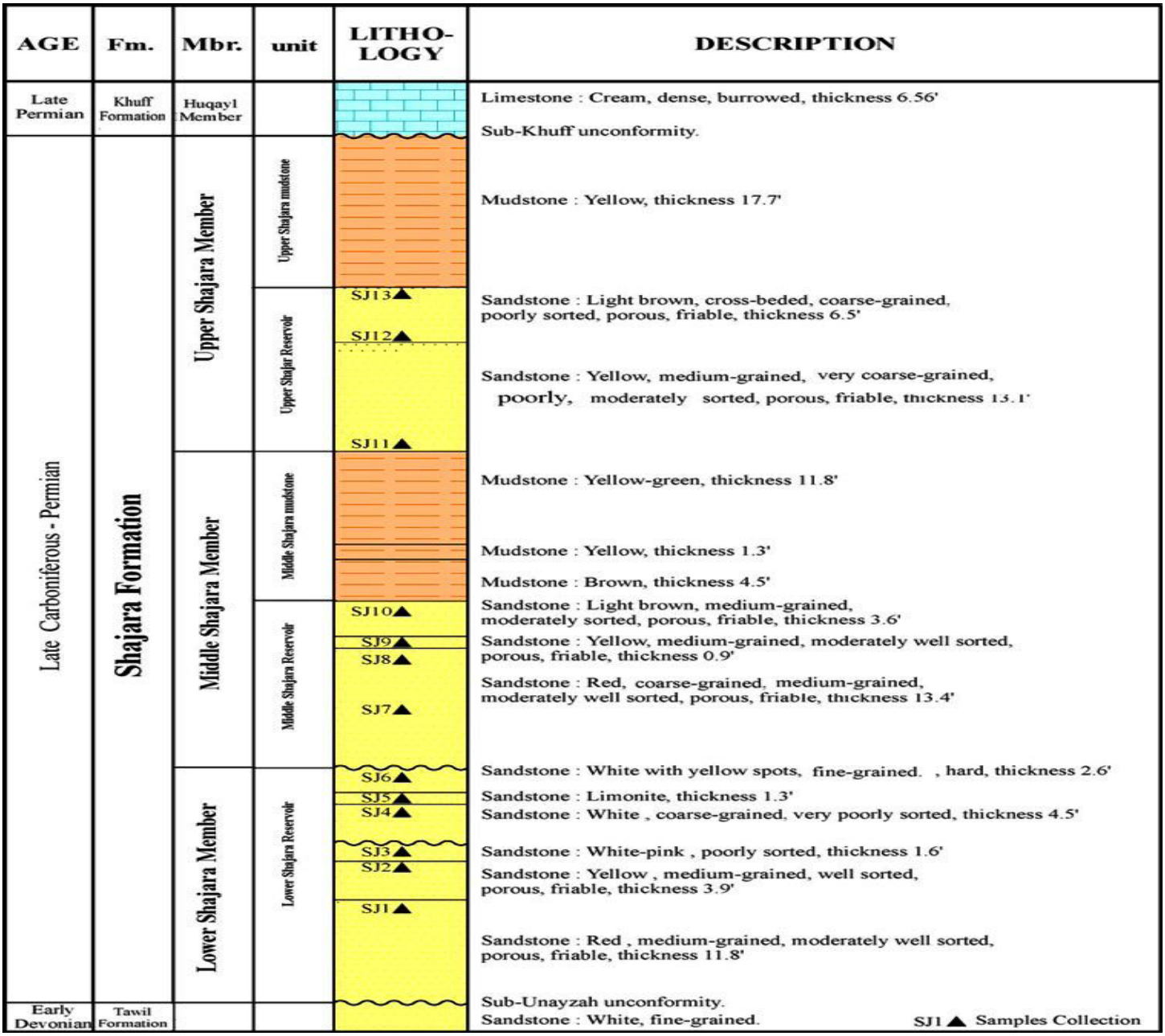

Figure 1: Surface type section of the Shajara Reservoirs of the Permo-Carboniferous Shajara Formation at latitude 26° 52' 17.4" longitude 43° 36' 18".

The Luminous efficacy can be scaled as

$$Sw = \left[\frac{Le^{\frac{1}{2}}}{Le_{max}^{\frac{1}{2}}}\right]^{[3-Df]} \quad 1$$

Where Sw the water saturation, Le luminous efficacy in lumen / watt, Le_{max} the maximum luminous in lumen / watt, Df the fractal dimension

Equation 1 can be proofed from

$$LP = L \times SA \times A \quad 2$$

Where LP the luminous power in lumen, L the luminance in lumen / (square radian × square meter), SA the solid angle in square radian, A the projected area in square meter.

The luminous power can also be scaled as

$$LP = RP \times Le \quad 3$$

Where LP the luminous power in lumen, RP the radiant power in watt, Le the luminous efficacy in lumen / watt.

Insert equation 3 into equation 2

$$RP \times Le = L \times SA \times A \quad 4$$

The area A can be scaled as

$$A = 4 \times 3.14 \times r^2 \quad 5$$

Where A the area in square meter, r the pore radius in meter

Insert equation 5 into equation 4

$$RP \times Le = L \times SA \times 4 \times 3.14 \times r^2 \quad 6$$

The maximum pore radius can be scaled as

$$RP \times Le_{max} = L \times SA \times 4 \times 3.14 \times r^2{}_{max} \quad 7$$

Divide equation 6 by equation 7

$$\left[\frac{RP \times Le}{RP \times Le_{max}}\right] = \left[\frac{L \times SA \times 4 \times 3.14 \times r^2}{L \times SA \times 4 \times 3.14 \times r^2{}_{max}}\right] \quad 8$$

Equation 8 after simplification will be

$$\left[\frac{Le}{Le_{max}}\right] = \left[\frac{r^2}{r^2{}_{max}}\right] \quad 9$$

Take the square root of equation9

$$\sqrt{\left[\frac{Le}{Le_{max}}\right]} = \sqrt{\left[\frac{r^2}{r^2{}_{max}}\right]} \quad 10$$

Equation 10 after simplification will be

$$\left[\frac{Le^{\frac{1}{2}}}{Le_{max}^{\frac{1}{2}}}\right] = \left[\frac{r}{r_{max}}\right] \quad 11$$

Take the logarithm of equation 11

$$\log\left[\frac{Le^{\frac{1}{2}}}{Le_{max}^{\frac{1}{2}}}\right] = \log\left[\frac{r}{r_{max}}\right] \quad 12$$

$$But, \log\left[\frac{r}{r_{max}}\right] = \frac{\log Sw}{[3-Df]} \quad 13$$

Insert equation 13 into equation 12

$$\frac{\log Sw}{[3-Df]} = \log\left[\frac{Le^{\frac{1}{2}}}{Le_{max}^{\frac{1}{2}}}\right] \quad 14$$

Equation 14 after log removal will become

$$Sw = \left[\frac{Le^{\frac{1}{2}}}{Le_{max}^{\frac{1}{2}}}\right]^{[3-Df]} \quad 15$$

Equation 15 the proof of equation 1 which relates the water saturation, luminous efficacy, maximum luminous efficacy, and the fractal dimension.

The capillary pressure can be scaled as

$$Sw = [Df - 3] \times Pc \times constant \quad 16$$

Where Sw the water saturation, Pc the capillary pressure and Df the fractal dimension.

Results and Discussion

Based on field observation the Shajara Reservoirs of the Permo-Carboniferous Shajara Formation were divided here into three units as described in (Figure1). These units from bottom to top are: Lower Shajara Reservoir, Middle Shajara reservoir, and Upper Shajara Reservoir. Their attained results of the luminous efficacy fractal dimension and capillary pressure fractal dimension are shown in (Table 1). Based on the achieved results it was found that the luminous efficacy fractal dimension is equal to the capillary pressure fractal dimension. The maximum value of the fractal dimension was found to be 2.7872 allocated to sample SJ13 from the Upper Shajara Reservoir as verified in (Table 1). Whereas the minimum value of the fractal dimension 2.4379 was reported from sample SJ3 from the Lower Shajara reservoir as shown in (Table 1). The Luminous efficacy fractal dimension and capillary pres-

sure fractal dimension were detected to increase with increasing permeability as proofed in (Table 1) owing to the possibility of having interconnected channels.

Formation	Reservoir	Sample	Porosity %	k (md)	Positive slope of the first procedure Slope=3-Df	Negative slope of the second procedureSlope=Df-3	Luminous efficacy fractal dimension	Capillary pressure fractal dimension
Permo-Carboniferous Shajara Formation	Upper Shajara Reservoir	SJ13	25	973	0.2128	-0.2128	2.7872	2.7872
		SJ12	28	1440	0.2141	-0.2141	2.7859	2.7859
		SJ11	36	1197	0.2414	-0.2414	2.7586	2.7586
	Middle Shajara Reservoir	SJ9	31	1394	0.2214	-0.2214	2.7786	2.7786
		SJ8	32	1344	0.2248	-0.2248	2.7752	2.7752
		SJ7	35	1472	0.2317	-0.2317	2.7683	2.7683
	Lower Shajara Reservoir	SJ4	30	176	0.3157	-0.3157	2.6843	2.6843
		SJ3	34	56	0.5621	-0.5621	2.4379	2.4379
		SJ2	35	1955	0.2252	-0.2252	2.7748	2.7748
		SJ1	29	1680	0.2141	-0.2141	2.7859	2.7859

Table 1: Petrophysical model showing the three Shajara Reservoir Units with their corresponding values of luminous efficacy fractal dimension and capillary pressure fractal dimension.

The Lower Shajara reservoir was symbolized by six sandstone samples (Figure 1), four of which label as SJ1, SJ2, SJ3 and SJ4 were carefully chosen for capillary pressure measurement as proven in (Table 1). Their positive slopes of the first procedure log of the Luminous efficacy to maximum Luminous efficacy versus log wetting phase saturation (Sw) and negative slopes of the second procedure log capillary pressure (Pc) versus log wetting phase saturation (Sw) are clarified in (Figures 2-5) and (Table 1). Their Luminous efficacy fractal dimension and capillary pressure fractal dimension values are revealed in (Table 1). As we proceed from sample SJ2 to SJ3 a pronounced reduction in permeability due to compaction was described from 1955 md to 56 md which reflects decrease in Luminous efficacy fractal dimension from 2.7748 to 2.4379 as quantified in (Table 1). Again, an increase in grain size and permeability was proved from sample SJ4 whose luminous efficacy fractal dimension and capillary pressure fractal dimension was found to be 2.6843 as described in (Table 1).

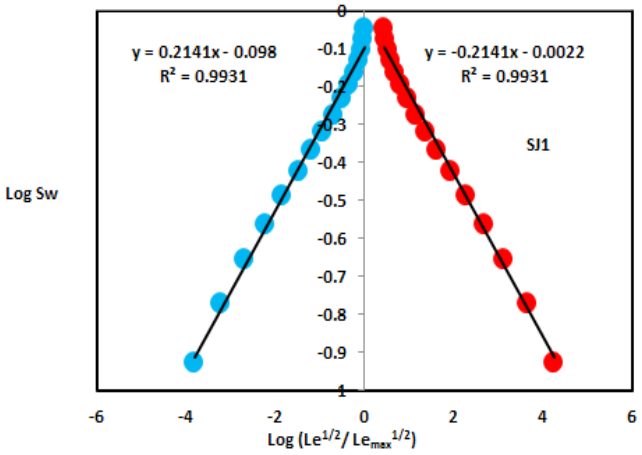

Figure 2: Log (Le1/2/Le1/2max) & log pc versus log Sw for sample SJ1.

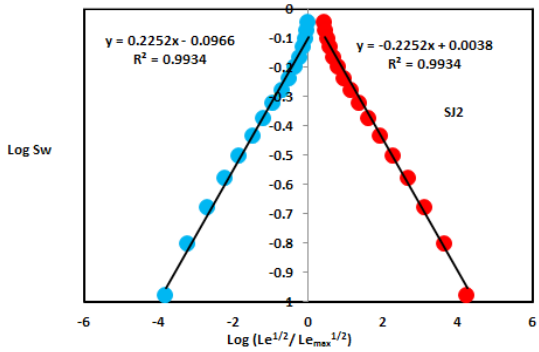

Figure 3: Log (Le1/2/Le1/2max) & log pc versus log Sw for sample SJ2.

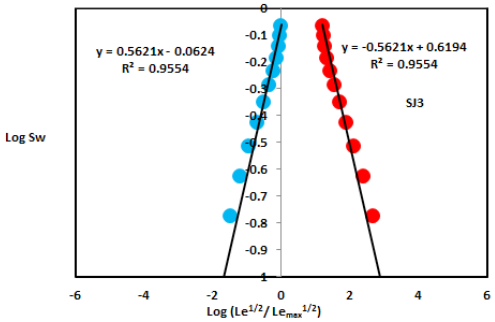

Figure 4: Log (Le1/2/Le1/2max) & log pc versus log Sw for sample SJ3.

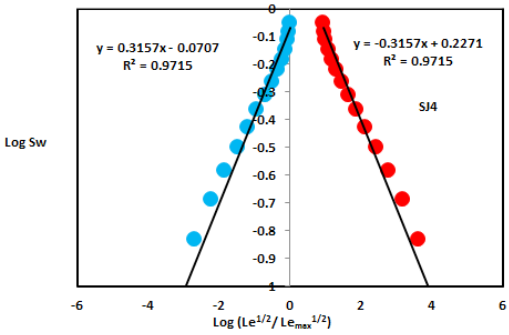

Figure 5: Log (Le1/2/Le1/2max) & log pc versus log Sw for sample SJ4.

In contrast, the Middle Shajara reservoir which is separated from the Lower Shajara reservoir by an unconformity surface as revealed in (Figure 1). It was nominated by four samples (Figure 1), three of which named as SJ7, SJ8, and SJ9 as illuminated in (Table1) were chosen for capillary measurements as described in (Table 1). Their positive slopes of the first procedure and negative slopes of the second procedure are shown in (Figures 6-8) (Table 1). Furthermore, their Luminous efficacy fractal dimensions and capillary pressure fractal dimensions show similarities as defined in (Table 1). Their fractal dimensions are higher than those of samples SJ3 and SJ4 from the Lower Shajara Reservoir due to an increase in their permeability as explained in (Table 1).

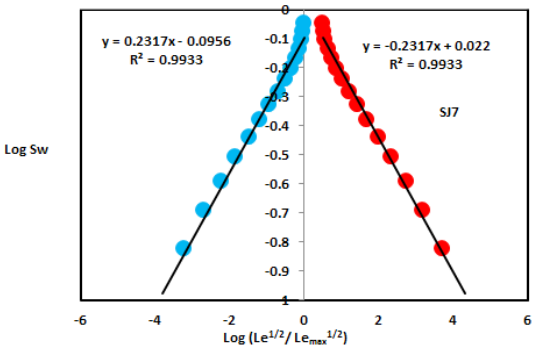

Figure 6: Log (Le1/2/Le1/2max) & log pc versus log Sw for sample SJ7.

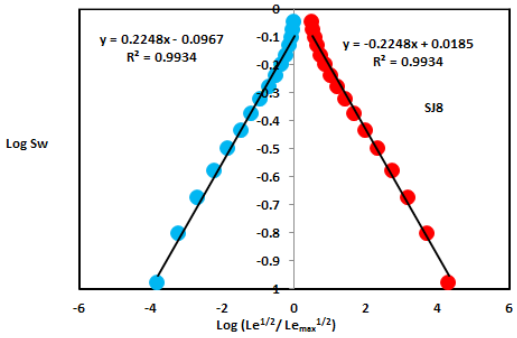

Figure 7: Log (Le1/2/Le1/2max) & log pc versus log Sw for sample SJ8.

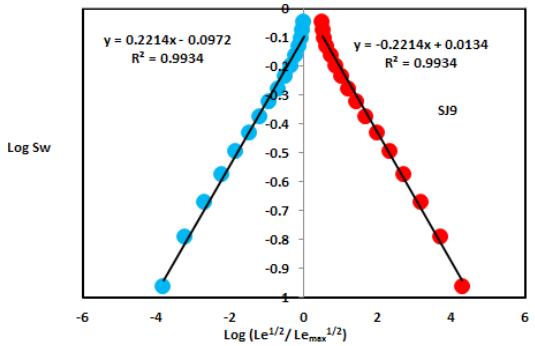

Figure 8: Log (Le1/2/Le1/2max) & log pc versus log Sw for sample SJ9.

On the other hand, the Upper Shajara reservoir was separated from the Middle Shajara reservoir by yellow green mudstone as shown in (Figure 1). It is defined by three samples so called SJ11, SJ12, SJ13 as explained in (Table 1). Their positive slopes of the first procedure and negative slopes of the second procedure are displayed in (Figures 9-11) and (Table 1). Moreover, their lu-

minous efficacy fractal dimension and capillary pressure fractal dimension are also higher than those of sample SJ3 and SJ4 from the Lower Shajara Reservoir due to an increase in their permeability as simplified in (Table 1).

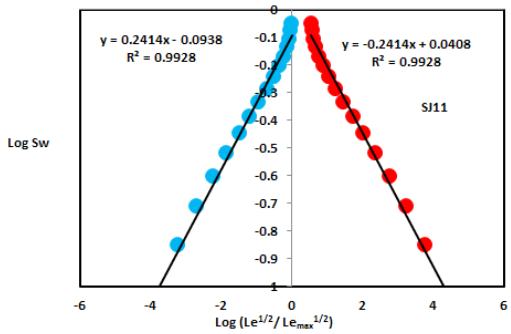

Figure 9: Log (Le1/2/Le1/2max) & log pc versus log Sw for sample SJ11.

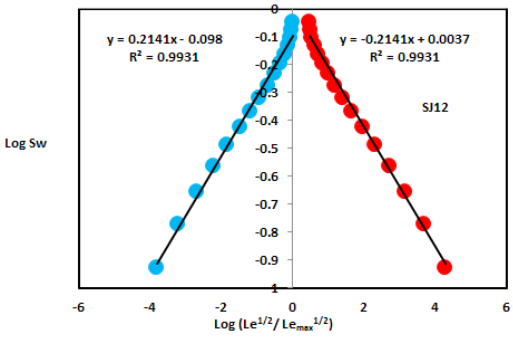

Figure 10: Log (Le1/2/Le1/2max) & log pc versus log Sw for sample SJ12.

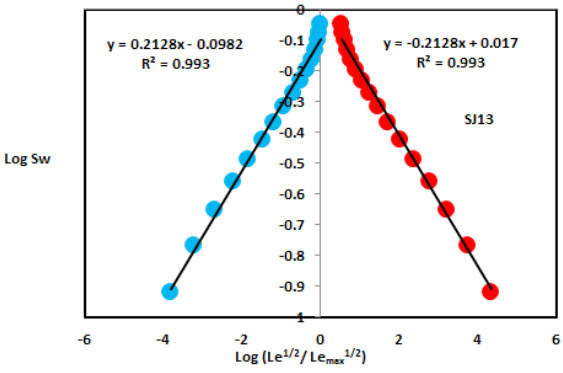

Figure 11: Log (Le1/2/Le1/2max) & log pc versus log Sw for sample SJ13.

Overall a plot of positive slope of the first procedure versus negative slope of the second procedure as described in (Figure 12) reveals three permeable zones of varying Petrophysical properties. These reservoir zones were also confirmed by plotting luminous efficacy fractal dimension versus capillary pressure fractal dimension as described in (Figure 13). Such variation in fractal dimension can account for heterogeneity which is a key parameter in reservoir quality assessment.

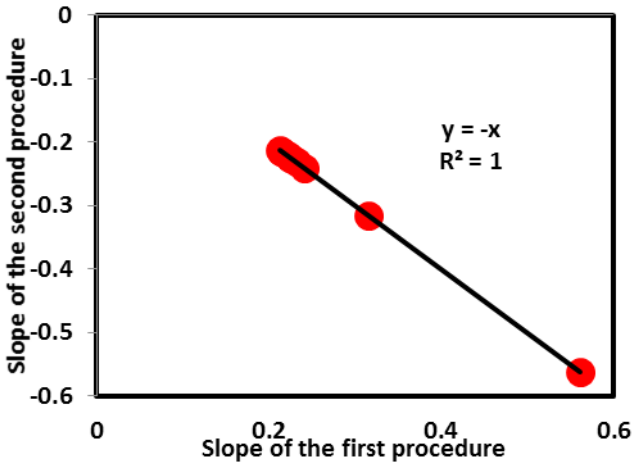

Figure 12: Slope of the first procedure versus slope of the second procedure.

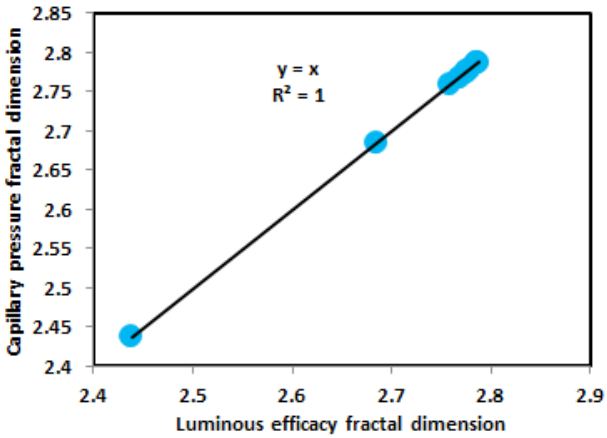

Figure 13: Luminous efficacy fractal dimension versus capillary pressure fractal dimension.

Conclusion

The sandstones of the Shajara Reservoirs of the permo-Carboniferous Shajara Formation were divided here into three units based on luminous efficacy fractal dimension. The Units from base to top are: Lower Shajara Luminous Efficacy Fractal Dimension Unit, Middle Shajara Luminous Efficacy Fractal Dimension Unit, and Upper Shajara Luminous Efficacy Fractal Dimension Unit. These units were also proved by capillary pressure fractal dimension. The fractal dimension was found to increase with increasing grain size and permeability owing to possibility of having interconnected channels.

Acknowledgement

The author would to thank King Saud University, college of Engineering, Department of Petroleum and Natural Gas Engineering, Department of Chemical Engineering, Research Centre at College of Engineering, College of science, Department of Geology, and King Abdullah Institute for research and Consulting Studies for their supports.

References

1. Frenkel, J. (1944) On the theory of seismic and seismoelectric phenomena in a moist soil. Journal of physics 3: 230-241.
2. Li K, Williams W (2007) Determination of capillary pressure function from resistivity data. Transport in Porous Media 67: 1-15.
3. Revil A, Jardani A (2010) Seismoelectric response of heavy oil reservoirs: theory and numerical modelling. Geophys J Int 180:781-797.
4. Dukhin A, Goetz P, Thommes M (2010) Seismoelectric effect: a non-isochoric streaming current.1 Experiment. Journal of Colloid Interface Science 345: 547-553.
5. Guan W, Hu H, Wang Z (2012) Permeability inversion from low-frequency seismoelectric logs in fluid- saturated porous formations Geophysical Prospecting 61: 120-133.
6. Hu H, Guan W, Zhao W (2012) Theoretical studies of permeability inversion from seismoelectric logs. Geophysical Research Abstracts.
7. Borde C, S´en´echal P, Barri`ere J, Brito D, Normandin E, et al. (2015) Impact of water saturation on seismoelectric transfer functions: a laboratory study of co-seismic phenomenon. Geophysical Journal International 200:1317-1335.
8. Jardani A, Revil A (2015) Seismoelectric couplings in a poroelastic material containing two immiscible fluid phases. Geophysical Journal International 202: 850-870.
9. Holzhauer J, Brito D, Bordes C, Brun Y, Guatarbes B (2016) Experimental quantification of the seismoelectric transfer function and its dependence on conductivity and saturation in loose sand. Geophysical Prospecting 65:1097-1120.
10. Ping R, Wei JX, Rang D, Ding PB, Liu AC (2016) Experimental research on seismoelectric effects in sandstone. Applied Geophysics 13: 425-436.
11. Djuraev U, Jufar SR, Vasant P (2017) Numerical Study of frequency-dependent seismo electric coupling in partially-saturated porous media. MATEC Web of Conferences 87,0200.
12. Alkhidir KEME (2017) Pressure head fractal dimension for characterizing Shajara Reservoirs of the Shajara Formation of the Permo-Carboniferous Unayzah Group, Saudi Arabia. Archives of Petroleum and Environmental Biotechnology 2:1-7.
13. Al-Khidir KE (2018) On Similarity of Pressure Head and Bubble Pressure Fractal Dimensions for Characterizing Permo-Carboniferous Shajara Formation, Saudi Arabia. Journal of Industrial Pollution and Toxicity 1: 1-10.
14. Alkhidir KEME (2018) Geometric relaxation time of induced polarization fractal dimension for characterizing Shajara Reservoirs of the Shajara Formation of the Permo-Carboniferous Unayzah Group, Saudi Arabia. Scifed Journal of Petroleum 21: 1-6.
15. Alkhidir KEME (2018) Geometric relaxation time of induced polarization fractal dimension for characterizing Shajara Reservoirs of the Shajara formation of the Permo-Carboniferous Unayzah Group-Permo. International Journal of Petrochemistry and Research 2: 105-108.